5.1.3.7.2. *Reflection geometry*

In this case (Fig. 5.1.3.5) $S(\gamma_h)$ is now -1 and (5.1.3.10) may be written

$$\xi_j = S(C)\left[\eta \pm (\eta^2 - 1)^{1/2}\right]/|\gamma|^{1/2}. \qquad (5.1.3.12)$$

Now, let I_1 and I_2 be the points of the dispersion surface where the tangent is parallel to the normal to the crystal surface, and further let I_{o1}, I_{h1}, I' and I_{o2}, I_{h2}, I'' be the intersections of these two tangents with T_o, T_h and T'_o, respectively. For an incident wave of wavevector **OM** where M lies between I' and I'', the normal to the crystal surface drawn from M has no real intersection with the dispersion surface and $\overline{I'I''}$ defines the total-reflection domain. The tie points I_1 and I_2 correspond to $\eta = -1$ and $\eta = +1$, respectively, the extinction distance $\Lambda_L = 1/\overline{I_{o1}I_{h1}}$, the width of the total-reflection domain $2\delta = \overline{I_{o1}I_{o2}}/k = \overline{I'I''}/k$ and the deviation parameter $\eta = -\overline{M_oM_h}/\overline{I_{o1}I_{h1}}$, where M_o and M_h are the intersections with T_o and T_h of the normal to the crystal surface drawn from the extremity of any incident wavevector **OM**.

5.1.4. Standing waves

The various waves in a wavefield are coherent and interfere. In the two-beam case, the intensity of the wavefield, using (5.1.2.14) and (5.1.2.24), is

$$|D|^2 = |D_o|^2 \exp(4\pi \mathbf{K}_{oi} \cdot \mathbf{r}) \times [1 + |\xi|^2 + 2C|\xi| \cos 2\pi(\mathbf{h} \cdot \mathbf{r} + \Psi)], \qquad (5.1.4.1)$$

where Ψ is the phase of ξ,

$$\xi = |\xi| \exp(i\Psi). \qquad (5.1.4.2)$$

Equation (5.1.4.1) shows that the interference between the two waves is the origin of *standing waves*. The corresponding nodes lie on planes such that $\mathbf{h} \cdot \mathbf{r}$ is a constant. These planes are therefore parallel to the diffraction planes and their periodicity is equal to d_{hkl} (defined in the caption for Fig. 5.1.2.1*a*). Their position within the unit cell is given by the value of the phase Ψ.

In the Laue case, Ψ is equal to $\pi + \varphi_h$ for branch 1 and to φ_h for branch 2, where φ_h is the phase of the structure factor, (5.1.2.6). This means that the *nodes* of standing waves lie on the maxima of the *hkl* Fourier component of the electron density for branch 1 while the *anti-nodes* lie on the maxima for branch 2.

In the Bragg case, Ψ varies continuously from $\pi + \varphi_h$ to φ_h as the angle of incidence is varied from the low-angle side to the high-angle side of the reflection domain by rocking the crystal. The nodes lie on the maxima of the *hkl* Fourier components of the electron density on the low-angle side of the rocking curve. As the crystal is rocked, they are progressively shifted by half a lattice spacing until the anti-nodes lie on the maxima of the electron density on the high-angle side of the rocking curve.

Standing waves are the origin of the phenomenon of anomalous absorption, which is one of the specific properties of wavefields (Section 5.1.5). Anomalous scattering is also used for the location of atoms in the unit cell at the vicinity of the crystal surface: when X-rays are absorbed, fluorescent radiation and photoelectrons are emitted. Detection of this emission for a known angular position of the crystal with respect to the rocking curve and therefore for a known value of the phase Ψ enables the emitting atom within the unit cell to be located. The principle of this method is due to Batterman (1964, 1969). For reviews, see Golovchenko *et al.* (1982), Materlik & Zegenhagen (1984), Kovalchuk & Kohn (1986), Bedzyk (1988), Authier (1989), and Zegenhagen (1993).

5.1.5. Anomalous absorption

It was shown in Section 5.1.2.2 that the wavevectors of a given wavefield all have the same imaginary part (5.1.2.17) and therefore the same absorption coefficient μ (5.1.2.19). Borrmann (1950, 1954) showed that this coefficient is much smaller than the normal one (μ_o) for wavefields whose tie points lie on branch 1 of the dispersion surface and much larger for wavefields whose tie points lie on branch 2. The former case corresponds to the *anomalous transmission effect*, or *Borrmann effect*. As in favourable cases the minimum absorption coefficient may be as low as a few per cent of μ_o, this effect is very important from both a fundamental and a practical point of view.

The physical interpretation of the Borrmann effect is to be found in the standing waves described in Section 5.1.4. When the nodes of the electric field lie on the planes corresponding to the maxima of the *hkl* component of the electron density, the wavefields are absorbed anomalously less than when there is no diffraction. Just the opposite occurs for branch 2 wavefields, whose anti-nodes lie on the maxima of the electron density and which are absorbed more than normal.

The effective absorption coefficient μ is related to the imaginary part of the wavevectors through (5.1.2.19),

$$\mu = -4\pi\gamma_o K_{oi},$$

and to the imaginary part of the ratio of the amplitude of the reflected to the incident wave through

$$\mu = \mu_o - 4\pi X_{oi}, \qquad (5.1.5.1)$$

where X_{oi} is the imaginary part of X_o, which, using (5.1.2.24) and (5.1.3.10), is given by

$$X_o = R\lambda|C|S(\gamma_h)(F_hF_{\bar{h}})^{1/2} \times \{\eta \pm [\eta^2 + S(\gamma_h)]^{1/2}\}/\left[2\pi V(|\gamma|)^{1/2}\right]. \qquad (5.1.5.2)$$

Taking the upper sign (+) for the $\pm$ term corresponds to tie points on branch 1 and taking the lower sign $(-)$ corresponds to tie points on branch 2.

The calculation of the imaginary part X_{oi} is different in the Laue and in the Bragg cases. In the former case, the imaginary part of $(\eta^2 + 1)^{1/2}$ is small and can be approximated while in the latter, the imaginary part of $(\eta^2 - 1)^{1/2}$ is large when the real part of the deviation parameter, η_r, lies between 1 and -1, and cannot be calculated using the same approximation.

5.1.6. Intensities of plane waves in transmission geometry

5.1.6.1. *Absorption coefficient*

In transmission geometry, the imaginary part of X_o is small and, using a first-order approximation for the expansion of $(\eta^2 + 1)^{1/2}$, (5.1.5.1) and (5.1.5.2), the effective absorption coefficient in the absorption case is

$$\mu_j = \mu_o\left[\tfrac{1}{2}(1 + \gamma^{-1}). \mp \frac{(\eta_r/2)(1 - \gamma^{-1}) + |C|(\gamma^{-1})^{1/2}|F_{ih}/F_{io}| \cos\varphi}{(\eta_r^2 + 1)^{1/2}}\right], \qquad (5.1.6.1)$$

where $\varphi = \varphi_{rh} - \varphi_{ih}$ is the phase difference between F_{rh} and F_{ih} [equation (5.1.2.10)], the upper sign $(-)$ for the $\mp$ term corresponds to branch 1 and the lower sign (+) corresponds to branch 2 of the dispersion surface. In the symmetric Laue case ($\gamma = 1$, reflecting planes normal to the crystal surface), equation (5.1.6.1) reduces to

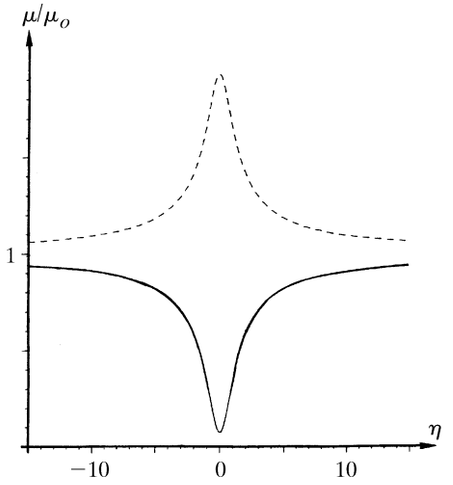

Fig. 5.1.6.1. Variation of the effective absorption with the deviation parameter in the transmission case for the 400 reflection of GaAs using Cu $K\alpha$ radiation. Solid curve: branch 1; broken curve: branch 2.

$$\mu_j = \mu_o \left[1 \mp \frac{|C||F_{ih}/F_{io}| \cos\varphi}{(\eta_r^2 + 1)^{1/2}} \right].$$

Fig. 5.1.6.1 shows the variations of the effective absorption coefficient μ_j with η_r for wavefields belonging to branches 1 and 2 in the case of the 400 reflection of GaAs with Cu $K\alpha$ radiation. It can be seen that for $\eta_r = 0$ the absorption coefficient for branch 1 becomes significantly smaller than the normal absorption coefficient, μ_o. The minimum absorption coefficient, $\mu_o(1 - |CF_{ih}/F_{io}| \cos\varphi)$, depends on the nature of the reflection through the structure factor and on the temperature through the Debye–Waller factor included in F_{ih} [equation (5.1.2.10*b*)] (Ohtsuki, 1964, 1965). For instance, in diamond-type structures, it is smaller for reflections with even indices than for reflections with odd indices. The influence of temperature is very important when $|F_{ih}/F_{io}|$ is close to one; for example, for germanium 220 and Mo $K\alpha$ radiation, the minimum absorption coefficient at 5 K is reduced to about 1% of its normal value, μ_o (Ludewig, 1969).

5.1.6.2. *Boundary conditions for the amplitudes at the entrance surface – intensities of the reflected and refracted waves*

Let us consider an infinite plane wave incident on a crystal plane surface of infinite lateral extension. As has been shown in Section 5.1.3, two wavefields are excited in the crystal, with tie points P_1 and P_2, and amplitudes D_{o1}, D_{h1} and D_{o2}, D_{h2}, respectively. Maxwell's boundary conditions (see Section A5.1.1.2 of the Appendix) imply continuity of the tangential component of the electric field and of the normal component of the electric displacement across the boundary. Because the index of refraction is so close to unity, one can assume to a very good approximation that there is continuity of the three components of both the electric field and the electric displacement. As a consequence, it can easily be shown that, *along the entrance surface*, for all components of the electric displacement

$$\begin{aligned} D_o^{(a)} &= D_{o1} + D_{o2} \\ 0 &= D_{h1} + D_{h2}, \end{aligned} \qquad (5.1.6.2)$$

where $D_o^{(a)}$ is the amplitude of the incident wave.

Using (5.1.3.11), (5.1.5.2) and (5.1.6.2), it can be shown that the *intensities* of the four waves are

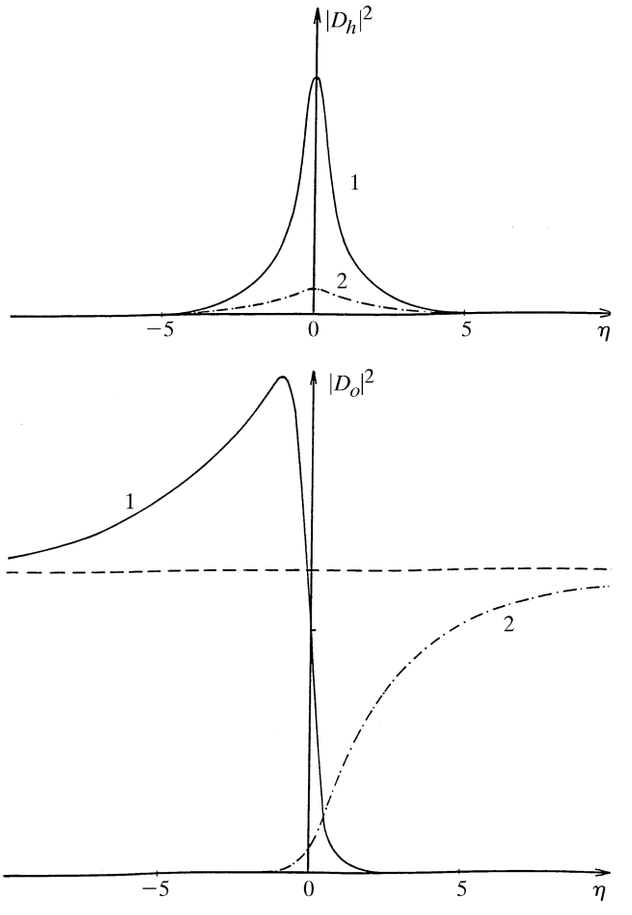

Fig. 5.1.6.2. Variation of the intensities of the reflected and refracted waves in an absorbing crystal for the 220 reflection of Si using Mo $K\alpha$ radiation, $t = 1$ mm ($\mu t = 1.42$). Solid curve: branch 1; dashed curve: branch 2.

$$\begin{aligned} |D_{oj}|^2 &= |D_o^{(a)}|^2 \exp(-\mu_j z/\gamma_o) \left[(1 + \eta_r^2)^{1/2} \mp \eta_r \right]^2 \\ &\quad \times [4(1 + \eta_r^2)]^{-1}, \\ |D_{hj}|^2 &= |D_o^{(a)}|^2 \exp(-\mu_j z/\gamma_o) |F_h/F_{\bar{h}}| [4\gamma(1 + \eta_r^2)]^{-1}; \end{aligned} \qquad (5.1.6.3)$$

top sign: $j = 1$; bottom sign: $j = 2$.

Fig. 5.1.6.2 represents the variations of these four intensities with the deviation parameter. Far from the reflection domain, $|D_{h1}|^2$ and $|D_{h2}|^2$ tend toward zero, as is normal, while

$$|D_{o1}|^2 \gg |D_{o2}|^2 \text{ for } \eta_r \Rightarrow -\infty,$$
$$|D_{o1}|^2 \ll |D_{o2}|^2 \text{ for } \eta_r \Rightarrow +\infty.$$

This result shows that the wavefield of highest intensity 'jumps' from one branch of the dispersion surface to the other across the reflection domain. This is an important property of dynamical theory which also holds in the Bragg case and when a wavefield crosses a highly distorted region in a deformed crystal [the so-called *interbranch scattering*: see, for instance, Authier & Balibar (1970) and Authier & Malgrange (1998)].

5.1.6.3. *Boundary conditions at the exit surface*

5.1.6.3.1. *Wavevectors*

When a wavefield reaches the exit surface, it breaks up into its two constituent waves. Their wavevectors are obtained by applying